Sodium Metal Oxyhalides Na $MOCl_4$ (M = Nb, Ta) with High Ionic Conductivities

Tong Zhao, ^{a,b} Bibek Samanta, ^{b,c} Xabier Martinez de Irujo Labalde, ^a Grace Whang, ^a Neelam Yadav, ^d Marvin A. Kraft, ^e Philipp Adelhelm, ^d Michael Ryan Hansen, ^c Wolfgang G. Zeier*^{a,e}

^aInstitute of Inorganic and Analytical Chemistry, University of Münster, 48149 Münster, Germany.

^bInternational Graduate School of Battery Chemistry, Characterization, Analysis, Recycling and Application (BACCARA), University of Münster, 48149 Münster, Germany.

^cInstitute of Physical Chemistry, University of Münster, 48149 Münster, Germany.

^dInstitut für Chemie, Humboldt Universität zu Berlin, Brook-Taylor-Str. 2, 12489 Berlin, Germany.

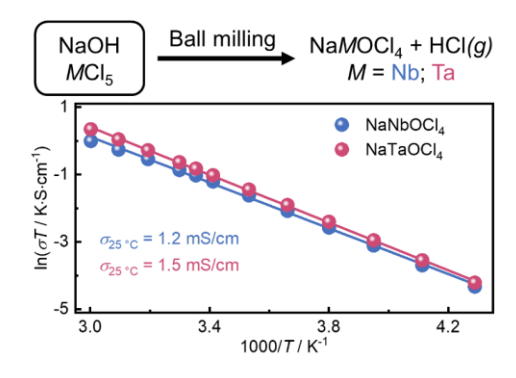
^eInstitut für Energie- und Klimaforschung (IEK), IEK-12: Helmholtz-Institut Münster, Forschungszentrum Jülich, 48149 Münster, Germany.

*wzeier@uni-muenster.de

Abstract

Halide-based ionic conductors have attracted a growing interest as solid electrolyte candidates because of their suggested electrochemical oxidation stability and deformability. However, most discovered sodium metal halides exhibit relatively low ionic conductivities. To address this, a new class of mechanochemically-stabilized, low-crystallinity sodium metal oxyhalides NaMOCl4 (*M* = Nb, Ta) is developed. By using the combination of scanning electron microscopy-energy dispersive X-ray spectroscopy, X-ray diffraction, pair distribution function analysis, Raman spectroscopy, and nuclear magnetic resonance spectroscopy, the composition and local structure of these oxyhalides are qualitatively explored. Notably, NaNbOCl4 and NaTaOCl4 exhibit high ionic conductivities of 1.2 and 1.5 mS·cm⁻¹, respectively. Although the instability of NaMOCl4 against Na excludes their use as standalone separators in solid-state sodium metal batteries, the successful operation of the solid-state battery employing NaTaOCl4 as the catholyte at room temperature demonstrates that NaMOCl4 is a promising catholyte material.

For table of contents only



For a zero-emission future, besides e-mobility and consumer electronics, commercial large-scale energy storage facilities based on numerous low-cost and safe batteries are needed. Sodium solidstate batteries are promising to meet these requirements because of the earth-abundance of sodium and the expected superior safety of solid-state batteries in comparison to conventional lithium ion batteries employing liquid electrolytes.²⁻⁵ As a core component of sodium solid-state batteries, ideal solid electrolytes require high ionic conductivity but low electronic conductivity, electrochemical stability under operation voltage, and chemical and mechanical compatibility with the active materials.^{5, 6} Sodium metal halides have attracted a growing interest as solid electrolyte candidates because of their suggested wider electrochemical stability windows in comparison to sulfides and better deformability in comparison to oxides.^{5, 7, 8} While there have been tremendous improvements in understanding the materials properties, so far the ionic conductivities of most sodium metal halides are still too low, even using the conventional cation doping strategies. For instance, Na_{2.25}Zr_{0.75}Y_{0.25}Cl₆ and Na_{2.4}Zr_{0.6}Er_{0.4}Cl₆ show the best ionic transport performance in the $Na_{2+x}Zr_{1-x}M_xCl_6$ (M = Y or Er) series, with ionic conductivities of only 6.6×10^{-5} and 3.5×10⁻⁵ S·cm⁻¹ respectively.^{8, 9} Nevertheless, a recent study shows that prolonging ball milling time can unexpectedly enhance the ionic conductivity of NaTaCl₆ up to 4 mS·cm⁻¹, which suggests that less-ordered halide-based sodium ionic conductors are more conductive. 10 Recently, lithium metal oxyhalides $LiMOCl_4$ (M = Nb, Ta) were synthesized by ball milling and subsequent annealing with precursors of LiOH and MCl₅, exhibiting high ionic conductivities of 10.4 $mS \cdot cm^{-1}$ for M = Nb and 12.4 $mS \cdot cm^{-1}$ for M = Ta respectively. To Following this work, Lin et al. synthesized a dual-anion sodium superionic glass 0.5Na₂O₂-TaCl₅ with an ionic conductivity of 4.6 mS·cm⁻¹, using a complex co-melting method. The solid-state battery employing it exhibits a stable cycling performance over 500 cycles. 12

Motivated by the outstanding transport properties of the lithium metal oxyhalides and their excellent performance in solid-state batteries, in this work, sodium metal oxyhalides $NaMOCl_4$ (M = Nb, Ta) with a low crystallinity are successfully synthesized by a simple ball milling method without need for a post-heat treatment. By using a combination of X-ray diffraction, pair distribution function (PDF) analyses, Raman spectroscopy, scanning electron microscopy-energy dispersive X-ray spectroscopy, and nuclear magnetic resonance spectroscopy (NMR), the local structure and composition of the amorphous oxyhalide $NaMOCl_4$ (M = Nb, Ta) are explored. The ionic conductivities of $NaNbOCl_4$ and $NaTaOCl_4$ reach 1.2 and 1.5 mS cm⁻¹ respectively. Although

their instability against Na metal precludes the possibility as standalone separators, the successful operation of the solid-state battery employing NaTaOCl₄ as the catholyte at room temperature indicates that this new class of fast sodium ionic conductors is a promising catholyte candidate for sodium solid-state batteries.

The sodium metal oxyhalides with targeted stoichiometry of Na $MOCl_4$ (M = Nb, Ta) are supposed to be mechanochemically synthesized (see Supporting Information) under the following chemical reaction NaOH + $MCl_5 \rightarrow NaMOCl_4 + HCl_{(g)}$, where M = Nb or Ta. To ensure the full reaction and degassing of protons as HCl, ¹H NMR spectroscopy was performed. Comparison of the ¹H magicangle spinning NMR spectra with and without samples (Figure S1) confirms the absence of residual protons in the milled products. To further validate the stoichiometries of the glassy products, energy dispersive X-ray spectroscopy in a scanning electron microscope was performed. As shown in *Figure S2-3*, the elements of Na, Nb (Ta), O and Cl homogeneously distribute within the samples. For both targeted compounds of NaNbOCl4 and NaTaOCl4, the atomic ratio of Na:M:Cl is roughly 1:1:4 (Figures S2f and S3f, Tables S1 and S2), with the oxygen content being off-stoichiometric as the light element content cannot be detected precisely. Since the existence of hydrogen in the ball milled products is excluded, the composition of the synthesized product, according to charge neutrality balancing, seems like NaNbOCl₄ and NaTaOCl₄ if all elements exist as their most stable ionic states. Thereby implying that a successful reaction occurs, similar to the reported reaction between LiOH and NbCl₅ (TaCl₅). However, the more accurate atomic composition of products is unclear at this stage. For more straightforward reading, the products are still denoted as NaNbOCl₄ and NaTaOCl₄ respectively.

To further investigate the structure of the obtained materials, X-ray diffraction is performed. The broad and merged reflections in the collected X-ray diffraction pattern of NaNbOCl₄ (*Figure 1a*) indicate its low crystallinity. Due to the low crystallinity, its phase cannot be indexed or matched to a previously reported compound in the Na-Nb-O-Cl phase space, and hence not allowing structure refinement. Therefore, as NaNbOCl₄ is not fully amorphous, the presence of a side phase cannot be fully excluded, although it is impossible to determine which reflection corresponds to the side phase because of the lack of structural information. However, NaOH seems not be present in line with ¹H NMR spectroscopy. ¹³ The X-ray diffraction pattern of NaTaOCl₄ (*Figure 1b*) reveals an almost fully amorphous phase, indicated by an extremely broad diffuse scattering

background visible, analogous to that of 0.5Na₂O₂-TaCl₅ glass prepared by co-melting at 450 °C.¹² A previous study indicates that TaCl₅ exhibits a strong capability to glassify salts,¹⁴ which likely also contributes to the amorphous nature of NaTaOCl₄. Thus, NaTaOCl₄ is more amorphous compared to NaNbOCl₄ synthesized with the same procedure. Due to this missing long-range order, it is impossible to attribute a long-range structure to NaTaOCl₄. This however also means, that there are no recognizable reflections in the pattern that can be matched to the precursors,¹³ again suggesting a full reaction.

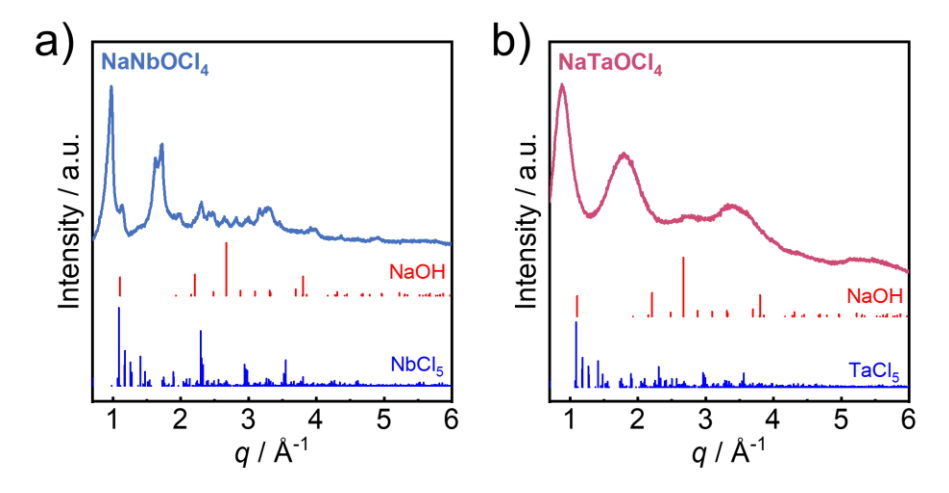


Figure 1. a) X-ray diffraction pattern of NaNbOCl₄ in comparison to reflections of precursors NaOH and NbCl₅, indicating a low crystallinity phase. The presence of a side phase in NaNbOCl₄ cannot be fully excluded. **b)** X-ray diffraction pattern of NaTaOCl₄ in comparison to reflections of precursors NaOH and TaCl₅. NaTaOCl₄ exhibits an almost fully amorphous phase.

Pair distribution function analysis is a powerful tool to determine the short-range ordering and local structure of materials whose coherence extends only a few nanometers using a measure of the probability of finding a pair of atoms (G(r)) separated by the distance r.¹⁵ Therefore, pair distribution function analyses are employed to make up for the deficiency of long-range ordering resolvable by Bragg diffraction to identify the local structure of the low-crystallinity NaMOCl₄. As shown in *Figures 2a-b*, the peaks of pair distribution functions of NaNbOCl₄ and NaTaOCl₄ dampen dramatically when the atomic distance r is over 5 Å, corroborating they have no long-range order, which agrees with the observation from X-ray diffraction patterns. However, the pair distribution functions obtained from different cut-off Q_{max} are strongly affected by Fourier termination ripples because of the low crystallinity and low scattering power of the synthesized

oxyhalides, leading to limited PDF data quality (Figure S4). Hence, only the signals at low r can be analyzed that correspond to a first and potentially second coordination sphere.

Comparison of the PDF data from NaNbOCl₄ with different Q_{max} shows that only the peak at ~2.4 Å is reliable and that the peak 3.9 Å is relatively stable when changing Q_{max} . In the case of NaTaOCl₄, a similar pair distribution function is observed, with only the signals at ~2.4 and 3.8 Å not changing significantly under different Q_{max} (Figure S4d). As the bond distances of NaTaOCl₄ PDF seems more stable and more intense and are here used for further qualitative discussion. A general idea of the coordination environment around the metals can be extracted by comparison with known compounds, as shown in *Figure 2c*, which may have similar local environments, such as NaOH, TaCl₅, TaOCl₃ and NaTaCl₆ (local environments of each metal schematically shown in Figure 2d). The strong peak at 2.4 Å can be assigned to Ta-Cl bond lengths, which matches with the Ta-Cl bond distance in TaCl₅ or TaOCl₃. The signal at 3.9 Å may be assigned to a Ta-Ta distance in analogy with TaCl₅ or TaOCl₃. In TaCl₅, two edge-shared [TaCl₆] octahedra form a [Ta₂Cl₁₀] bioctahedra with a Ta-Ta distance of ~3.9 Å. Similarly, in TaOCl₃, two edge-shared [TaCl₄O₂]³⁻ octahedra form a [Ta₂Cl₆O₄]⁴⁻ bi-octahedra or two oxygen anion-shared [TaCl₄O₂]³⁻ octahedra form a [Ta₂Cl₈O₃]⁴⁻ bi-octahedra, both with a distance of ~3.9 Å between two central tantalum cations. However, the other probably existing bond signals are not observed, such as Ta-O, Na-O and Na-Cl and hence marked in grey in *Figure 2c*. A potential reason may be the lower scattering form factor of Na and O compared to Ta and Cl atoms, or their signals are convoluted into Fourier ripples of PDF at ~1.8 and 3.1 Å. With these data, one may speculate that bi- $[TaCl_xO_{6-x}]^{(7-x)-}$ units, evolved from the [Ta₂Cl₁₀] bi-octahedra in the precursor TaCl₅, form a not very structurally correlated framework where the Na⁺ cations are randomly distributed in NaTaOCl₄. Moreover, we can infer a similar local arrangement for NaNbOCl₄ (Figure S5). At this stage, further discussion does not seem reasonable, as even a data analysis with the reverse Monte Carlo method would provide a local structure that cannot be fully corroborated. The actual local environments of Na and M in NaMOCl₄ may be different or more diverse since we can only compare the atom pair distances with those of the already known compounds. Nevertheless, the above discussion seems chemically reasonable within the measured data.

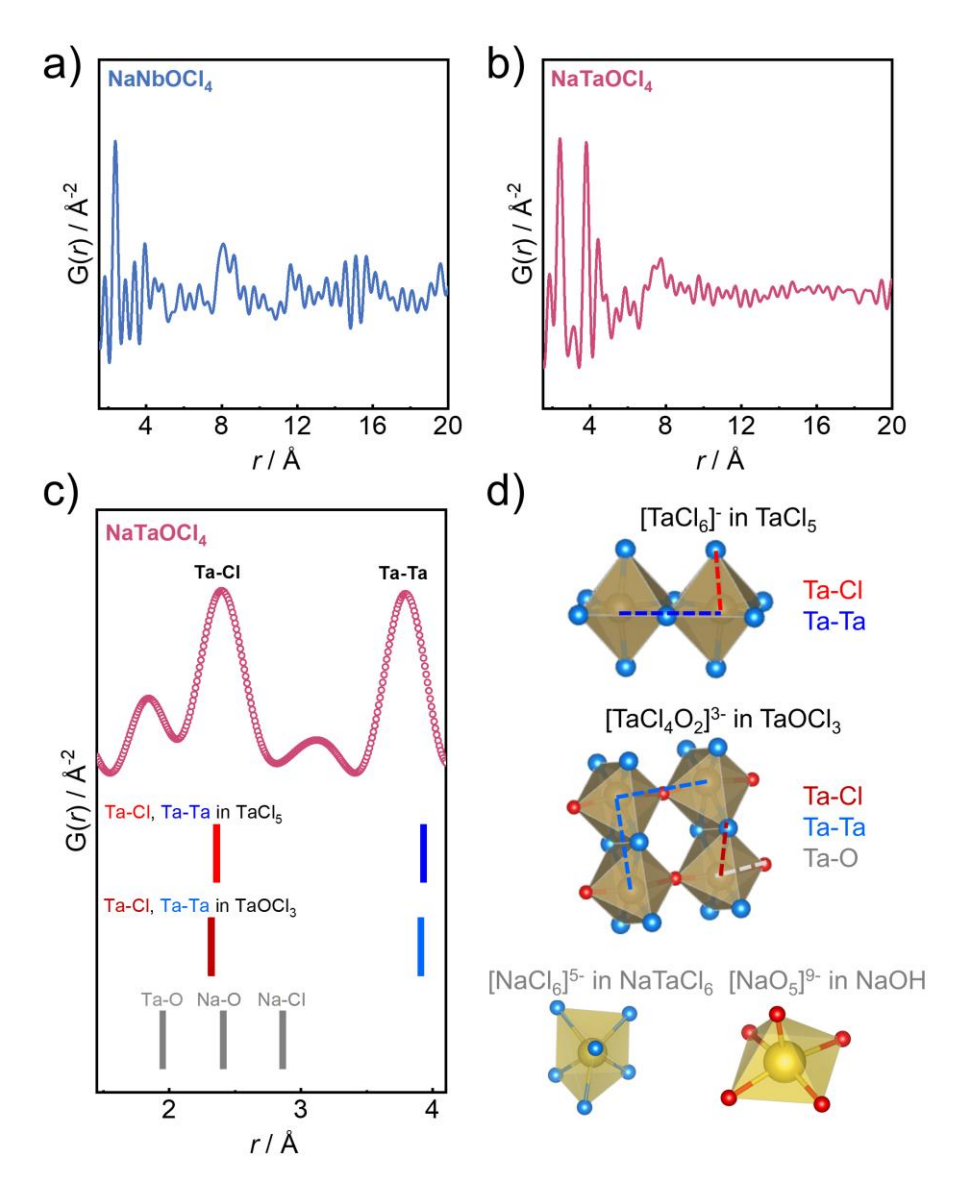


Figure 2. Pair distribution functions of **a)** NaNbOCl₄ and **b)** NaTaOCl₄. **c)** Comparison between pair distances (Ta-Cl and Ta-Ta pairs in TaCl₅, Ta-O, Ta-Cl and Ta-Ta pairs in TaOCl₃, Na-Cl pair in NaTaCl₆ and Na-O pair in NaOH) and measured pair distribution function of NaTaOCl₄. **d)** Schematically local environments of each metal used for pair distance comparison with the pair distribution function of NaTaOCl₄.

To further analyze the structural arrangement, Raman spectroscopy was used to determine their vibration modes. Even though several signals probably analogous to M-Cl vibrations (M = Nb, Ta) and Nb-O bond are observed ($Figure\ S6$), $^{16-20}$ the peak broadening and merging hinder further information extraction, making accurate analysis impossible. Nevertheless, it seems that together

with the PDF data the Raman spectra suggest not only M-Cl and M-M distances, but also M-O vibrations. However, no local environment information of sodium ion can be extracted from Raman spectroscopy here. Therefore, ²³Na magic angle spinning nuclear magnetic resonance was conducted to explore the local environment of Na⁺ in NaNbOCl₄ and NaTaOCl₄. For NaNbOCl₄, deconvolution of the room-temperature spectrum reveals two kinds of local environments of Na⁺ $(\delta(^{23}\text{Na}) = -11.46 \text{ ppm} \text{ and } -11.53 \text{ ppm} \text{ with an integral intensity ratio of } \sim 3:2), indicating either$ two distinct local environments in one phase or a possible side phase precipitating during ball milling. Corresponding low-temperature spectrum reveals peaks with a better separation ($\delta(^{23}\text{Na})$ = -11.96 ppm and -13.52 ppm) and their integral intensity ratio becomes $\sim 6:1$ (*Figure 3b*). This is a possible indication of chemical exchange between two different local environments of Na⁺, where the corresponding ²³Na signals get closer due to increased exchange with increasing temperature (and possibly leading to eventual coalescence at even higher temperature, when the crossover point is achieved). 21 For NaTaOCl₄, there is only one pronounced 23Na signal at -10.72 ppm in the room-temperature spectrum, indicating sole local environment of sodium ions (Figure 3c). The corresponding low-temperature ²³Na magic angle spinning nuclear magnetic resonance spectrum also only includes a single ²³Na resonance, which further solidifies this conclusion. Besides, the 23 Na resonance signal at ~ 7.3 ppm (marked with a solid triangle) in all spectra can be assigned to a small amount of NaCl impurity present in the samples. 21, 22

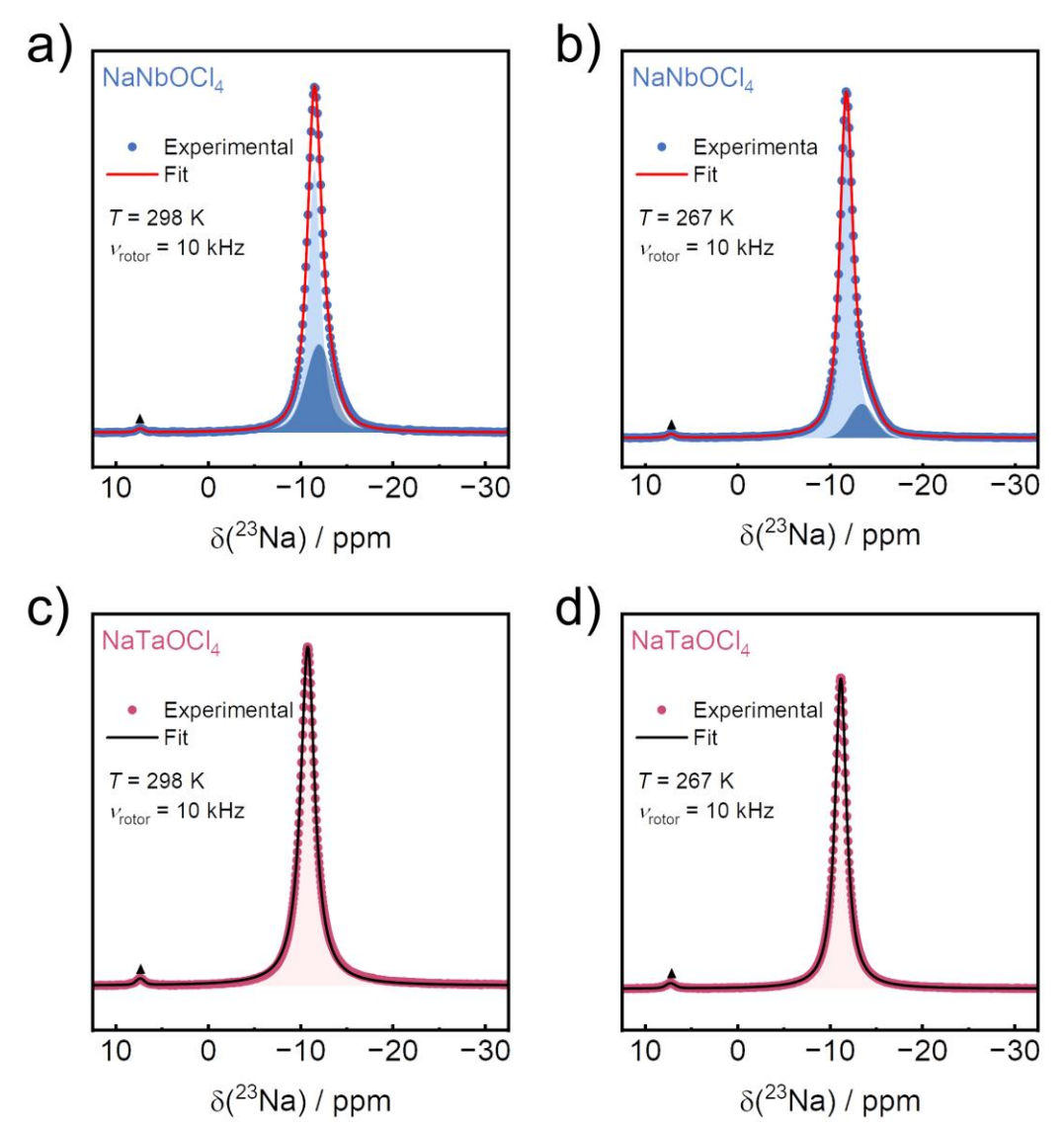


Figure 3. ²³Na magic angle spinning nuclear magnetic resonance spectra of NaNbOCl₄ measured at **a)** room temperature (~298 K) and **b)** low temperature (~267 K). The two deconvoluted ²³Na signals of NaNbOCl₄ are marked with light and dark blue shades, respectively. ²³Na magic angle spinning nuclear magnetic resonance spectra of NaTaOCl₄ measured at **c)** room temperature (~298 K) and **d)** low temperature (~267 K). The only ²³Na signal of NaTaOCl₄ is marked with a light red shade. The solid triangle (\triangle) indicates signal of impurity NaCl.

While structural information remains limited as described, the ionic conductivity was evaluated by temperature-dependent electrochemical impedance spectroscopy to investigate the transport property of NaNbOCl₄ and NaTaOCl₄. All impedance spectra of NaNbOCl₄ and NaTaOCl₄ can be fit with an equivalent circuit model (the inset of *Figure 4a*) consisting of a parallel resistor-constant

phase element (CPE) combination representing ion transport behavior of the measured sample, in series with another CPE representing the ion blocking behavior of the stainless-steel electrodes. The resolved Brug capacitances are around $\sim 10^{-11}$ F, indicating it cannot exclude either ordered bulk or disordered grain boundary contributions, ^{23,24} in line with the structural analyses above, thus the obtained resistances are evaluated to total ionic conductivities. The obtained room-temperature (25 °C) ionic conductivities (σ_{RT}) of NaNbOCl₄ and NaTaOCl₄ are 1.2 and 1.5 mS·cm⁻¹ respectively. As determined by the pair distribution function analyses, both NaNbOCl₄ and NaTaOCl₄ exhibit a high degree of structural disorder. Here, one may speculate that there are potentially different types of disorder possible in NaMOCl₄: 1) Na⁺ positional disorder and 2) polyhedral disorder, which may both lead to the low crystallinity of NaMOCl₄; and 3) anion site disorder between Cl and O. The potential structural disorders may be one of the factors contributing to the high ionic conductivities of NaMOCl₄, as previous studies have commonly observed that a less ordered structure facilitates Na+ movement in halide-based sodium ionic conductors. 10, 25, 26 The ionic conductivities of NaNbOCl₄ and NaTaOCl₄ are at least two orders of magnitude higher than that of pristine sodium metal chlorides (*Figures 4c*), such as Na₂ZrCl₆ ($\sim 1.8 \times 10^{-5} \text{ S} \cdot \text{cm}^{-1}$) and Na₃*M*Cl₆-type halides (e.g. $\sim 2.3 \times 10^{-8} \text{ S} \cdot \text{cm}^{-1}$ for $M = \text{In}, \sim 1.0 \times 10^{-9} \text{ S} \cdot \text{cm}^{-1}$ for M = Er), $^{9, 25}$, ²⁷ except the highly amorphous NaTaCl₆ synthesized under extreme ball milling conditions (~4 mS·cm⁻¹).¹⁰ The values are also much higher than that of cation substituted sodium chlorides, for instance, Na_{2.25}Zr_{0.75}Y_{0.25}Cl₆ and Na_{2.4}Zr_{0.6}Er_{0.4}Cl₆ with ionic conductivities of 6.6×10^{-5} and 3.5× 10⁻⁵ S·cm⁻¹.^{8, 9} Just mixing halogen in sodium metal halides (e.g. Na₃InCl_{6-x}Br_x) also cannot significantly enhance ionic conductivity.²⁸ However, the O and Cl dual anion systems beyond the pure halide system show ionic conductivities of over 1 mS·cm⁻¹, not only NaNbOCl₄ and NaTaOCl₄, but also 0.5Na₂O₂-TaCl₅ glass (4.6 mS·cm⁻¹), ¹² indicating the significance of extending composition systems of halide-based sodium ionic conductors. The activation energies (E_a) extracted from the linear Arrhenius fitting are 0.29(4) eV for NaNbOCl₄ and 0.31(2) eV for NaTaOCl₄. This is in a similar range to those observed in 0.5Na₂O₂-TaCl₅ glasses and lower than those generally observed in ternary sodium halides (~0.4 to 0.8 eV).^{8, 9, 12, 25, 27} Besides the ionic conductivities, the electronic conductivities (σ_e) of NaNbOCl₄ and NaTaOCl₄, determined by the direct-current polarization method, are $6.4(4) \times 10^{-10}$ and $3.2(2) \times 10^{-10}$ S·cm⁻¹ respectively (Figure S9). Such low electronic conductivities meet the requirement of solid electrolytes. 29, 30

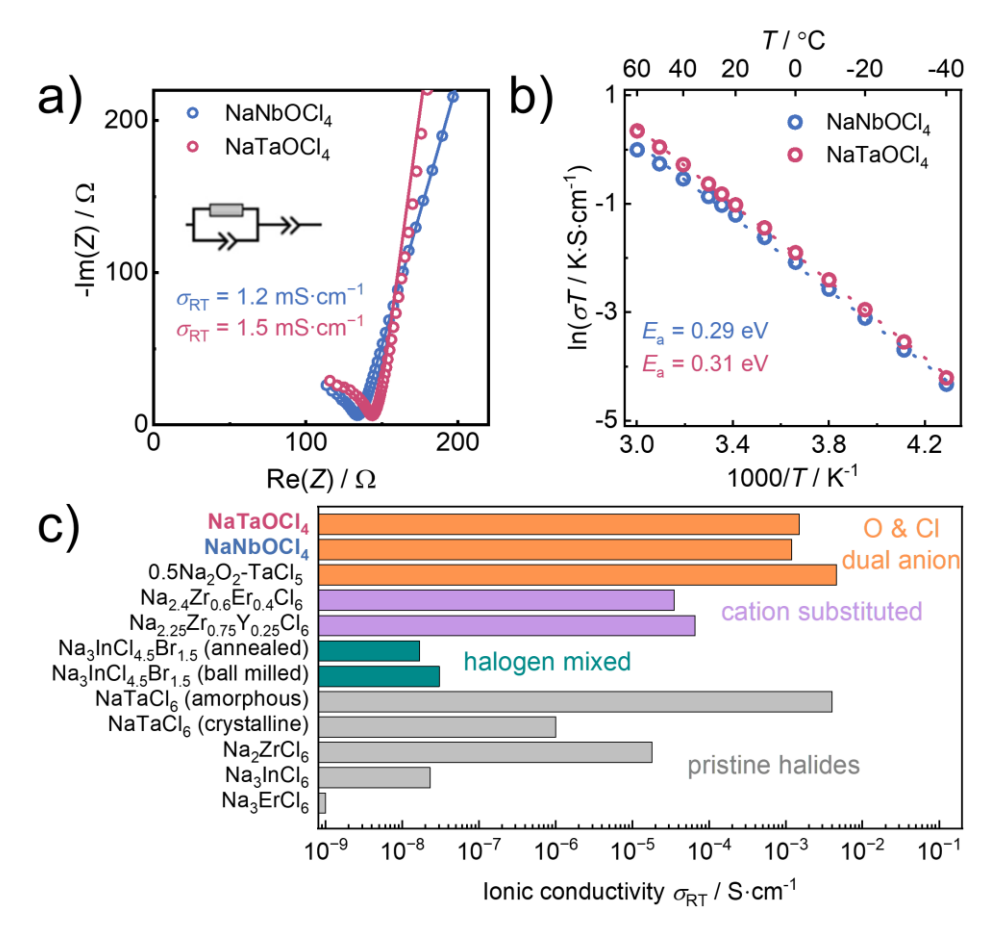


Figure 4. a) Nyquist plots of NaNbOCl₄ and NaTaOCl₄ measured at 25 °C. Inset: equivalent circuit model used for fitting impedance spectra. b) Arrhenius plots from the temperature dependent impedance of NaNbOCl₄ and NaTaOCl₄. c) Comparison of ionic conductivities of halide-based sodium ionic conductors with that of NaNbOCl₄ and NaTaOCl₄ (1.2 and 1.5 mS·cm⁻¹ respectively), including Na₃MCl₆-type halides (~2.3 × 10⁻⁸ S·cm⁻¹ for M = In, ~1.0 × 10⁻⁹ S·cm⁻¹ for M = Er), 9. 27 Na₂ZrCl₆ (~1.8 × 10⁻⁵ S·cm⁻¹), 25 crystalline NaTaCl₆ (~1.0 × 10⁻⁶ S·cm⁻¹), 10 highly amorphous NaTaCl₆ (~4 mS·cm⁻¹), 10 halogen-mixed Na₃InCl_{4.5}Br_{1.5} (~1.6 × 10⁻⁸ S·cm⁻¹ for the annealed, ~3.0 × 10⁻⁸ S·cm⁻¹ for the ball milled), 28 cation substituted sodium chlorides (Na_{2.25}Zr_{0.75}Y_{0.25}Cl₆ and Na_{2.4}Zr_{0.6}Er_{0.4}Cl₆ with ionic conductivities of 6.6 × 10⁻⁵ and 3.5 × 10⁻⁵ S·cm⁻¹), 8, 9 and 0.5Na₂O₂-TaCl₅ glass (4.6 mS·cm⁻¹). 12

Overall, this class of NaNbOCl₄ and NaTaOCl₄ shows one of the highest so-far found Na⁺ conductivities in halogen-containing ionic conductors. However, for the application as solid electrolytes they also require chemical and electrochemical stability against the electrodes if they are to be used as a separator.^{31, 32} To evaluate the chemical stability of the synthesized oxyhalides

against sodium metal, the time-dependent impedance spectra of Na|NaMOCl4|Na symmetric cells were measured (Figure S10). One can find two processes of impedance spectra that are significantly overlapping, which makes it hard to accurately fit the data, hence only total resistances can be extracted. The total resistance increases dramatically for both Na|NaNbOCl4|Na and Na|NaTaOCl₄|Na symmetric cells (*Figure 5a*), indicating that NaMOCl₄ is unstable against sodium metal. Even though the complex chemical reaction behavior cannot be properly resolved, in general, there are three different possible types of the interface/interphase between solid electrolyte and sodium metal in a Na|solid electrolyte|Na symmetric cell. (I) the solid electrolyte is stable against sodium metal and the total resistance of the symmetric cell remains at a steady value. (II) The solid electrolyte may decompose (e.g. being reduced) when in contact with sodium metal, leading to the formation of a mixed conducting interphase (MCI). If the ionic conductivity of MCI (σ_{MCI}) is greater than that of solid electrolyte (σ_{SE}), the total resistance of the symmetric cell assessed by impedance will decline. In contrast, the total resistance will increase when $\sigma_{MCI} < \sigma_{SE}$. Nevertheless, with the growth of MCI, the symmetric cell will short-circuit after some time as the MCI penetrates the solid electrolyte layer with a linear time dependency. (III) The solid electrolyte also reacts with sodium metal but forms a solid electrolyte interphase (SEI) which basically only conducts Na⁺. The change of impedance-assessed total resistance of the symmetric cell will depend on the competition between ionic conductivity of SEI (σ_{SEI}) and σ_{SE} too, but it may be steady ultimately since the electronic conductivity of SEI is low enough to limit the SEI growth to a thin film. 31, 33 In the case of Na|NaMOCl4|Na symmetric cells, their increasing total resistance indicates the formation of interphases between NaMOCl4 and Na which are less ionically conductive than NaMOCl₄. While an in-depth understanding of the reaction mechanism is beyond the scope of this work, one may speculate that NaMOCl₄ is reduced and decomposes to Na salts and/or Nb (Ta) salts or, eventually, to the metals. Additionally, the prediction from thermodynamic stabilities suggests that NaNbOCl₄ and Na metal form NaNbO₂, NaCl and metal Nb, while NaTaOCl₄ and Na metal form NaTaO₃, NaCl and metal Ta.³⁴ This prediction aligns with our chemical intuition. Based on the more linear growth rate of resistance, one can assume that a mixed conducting interphase is formed, rather than an SEI as an SEI should show parabolic, diffusion-controlled growth. Furthermore, the cycling (stripping and plating) performance of Na|NaMOCl₄|Na symmetric cells was also tested under 60 μA (~0.2 mA·cm⁻²) to further evaluate the impact of the electrochemical instability of NaMOCl₄ against Na, as shown in Figure S11. The continuous, rapid increase in the measured overpotential for both symmetric cells of NaNbOCl₄ and NaTaOCl₄, respectively,

indicates their electrochemical instability against Na metal.

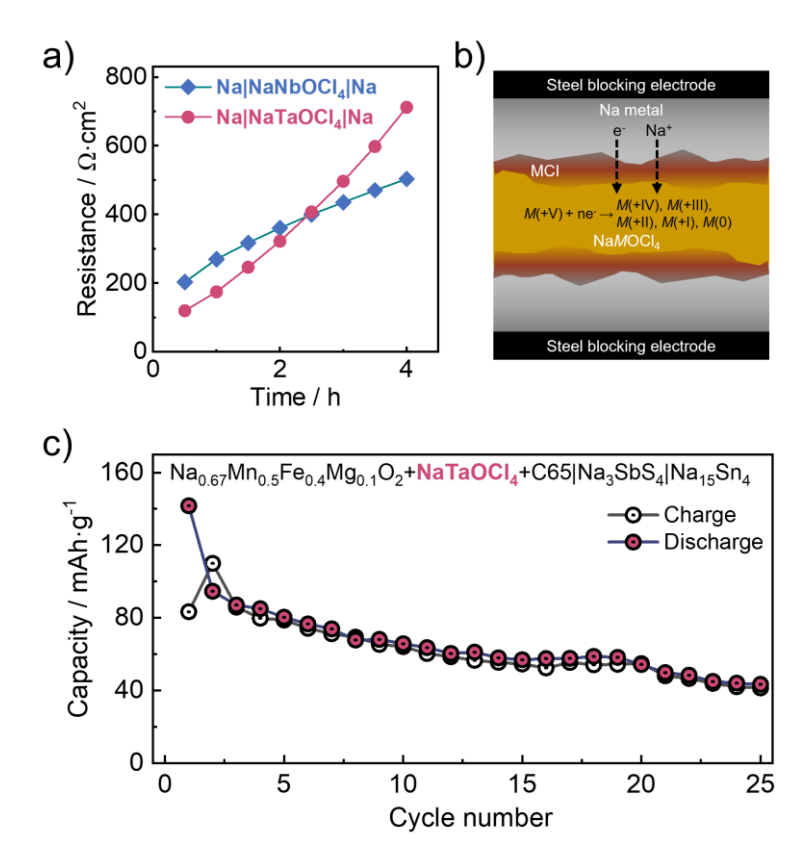


Figure 5. a) Total resistance evolutions of symmetric cells Na|NaNbOCl₄|Na and Na|NaTaOCl₄|Na, extracted from time-dependent impedance. b) Scheme of the mixed conducting interphase between sodium metal and NaMOCl₄ in Na|NaMOCl₄|Na symmetric cells. c) Cycling performance of the solid-state battery employing NaTaOCl₄ as catholyte. The battery was cycled at room temperature (~25°C) with an initial formation cycle at C/50, followed by cycling at C/30 within a voltage range of 1.5 - 4.2 V vs Na/Na⁺ (see the assembly and test procedures in the Supporting information).

Clearly, these findings exclude the possibility of using NaMOCl₄ as a standalone separator in solid-state sodium metal batteries; however, their use as catholytes still remains promising. To assess the feasibility of NaMOCl₄ catholytes, the cycling performance of the solid-state battery employing NaTaOCl₄ as the catholyte was tested at room temperature. As shown in *Figures 5c and S12*, the battery exhibits an initial fading in capacity, followed by a relatively stable cycling, demonstrating the potential of NaTaOCl₄ as the catholyte material.

In this work, mechanochemically stabilized sodium metal oxyhalides NaMOCl₄ (M = Nb, Ta) were successfully synthesized by ball milling. The as obtained NaNbOCl₄ and NaTaOCl₄ are low crystalline materials, exhibiting an ionic conductivity of 1.2 and 1.5 mS·cm⁻¹, respectively. Due to their fast degradation against Na-metal, their use as standalone separators in solid-state sodium metal batteries is restricted. Nevertheless, the successful operation of the solid-state battery employing NaTaOCl₄ as the catholyte at room temperature demonstrates the potential of NaMOCl₄ to be catholyte material. Going further, the structures of NaMOCl₄ need to be better understood to further improve their transport properties and even stability, as well as prospectively replacing tantalum and niobium with cheaper elements.

Acknowledgments

This work is funded by the Ministry of Culture and Science of the State North Rhine Westphalia in course of the International Graduate School of Battery Chemistry, Characterization, Analysis, Recycling and Application (BACCARA). The authors acknowledge financial support within the NATTER funded by Bundesministerium für Bildung und Forschung (BMBF project 03XP0525B). We further acknowledge funding from the Deutsche Forschungsgemeinschaft under project number 459785385.

Supporting Information

Experimental procedures, 1 H nuclear magnetic resonance measurement results of NaNbOCl₄ and NaTaOCl₄, scanning electron microscopy micrograph and energy dispersive X-ray spectroscopy mapping of NaNbOCl₄ and NaTaOCl₄, pair distribution functions of NaMOCl₄ with different cut-off Q_{max} , Raman spectra of NaMOCl₄, Nyquist plots of impedance data of NaNbOCl₄ and

NaTaOCl₄ measured from -40 to 60 °C, direct-current polarization curves and electronic conductivities of NaMOCl₄, time-dependent impedance measurements of symmetric cells Na|NaMOCl₄|Na, electrochemical cycling performance of symmetric cells Na|NaMOCl₄|Na, charge-discharge curves of the solid-state battery employing NaTaOCl₄ as catholyte.

Reference

- 1. Hirsh, H. S.; Li, Y.; Tan, D. H. S.; Zhang, M.; Zhao, E.; Meng, Y. S., Sodium-Ion Batteries Paving the Way for Grid Energy Storage. *Advanced Energy Materials* **2020**, *10*, 2001274.
- 2. Yang, H.-L.; Zhang, B.-W.; Konstantinov, K.; Wang, Y.-X.; Liu, H.-K.; Dou, S.-X., Progress and Challenges for All-Solid-State Sodium Batteries. *Advanced Energy and Sustainability Research* **2021**, *2*, 2000057.
- 3. Nayak, P. K.; Yang, L.; Brehm, W.; Adelhelm, P., From Lithium-Ion to Sodium-Ion Batteries: Advantages, Challenges, and Surprises. *Angew. Chem. Int. Ed. Engl.* **2018**, *57*, 102-120.
- 4. Janek, J.; Zeier, W. G., A solid future for battery development. *Nature Energy* **2016**, *1*, 16141.
- 5. Janek, J.; Zeier, W. G., Challenges in speeding up solid-state battery development. *Nature Energy* **2023**, *8*, 230-240.
- 6. Zheng, F.; Kotobuki, M.; Song, S.; Lai, M. O.; Lu, L., Review on solid electrolytes for all-solid-state lithium-ion batteries. *J. Power Sources* **2018**, *389*, 198-213.
- 7. Qie, Y.; Wang, S.; Fu, S.; Xie, H.; Sun, Q.; Jena, P., Yttrium—Sodium Halides as Promising Solid-State Electrolytes with High Ionic Conductivity and Stability for Na-Ion Batteries. *The journal of physical chemistry letters* **2020**, *11*, 3376-3383.
- 8. Wu, E. A.; Banerjee, S.; Tang, H.; Richardson, P. M.; Doux, J.-M.; Qi, J.; Zhu, Z.; Grenier, A.; Li, Y.; Zhao, E.; Deysher, G.; Sebti, E.; Nguyen, H.; Stephens, R.; Verbist, G.; Chapman, K. W.; Clément, R. J.; Banerjee, A.; Meng, Y. S.; Ong, S. P., A stable cathode-solid electrolyte composite for high-voltage, long-cycle-life solid-state sodium-ion batteries. *Nature Communications* **2021**, *12*, 1256.
- 9. Schlem, R.; Banik, A.; Eckardt, M.; Zobel, M.; Zeier, W. G., Na3–xEr1–xZrxCl6—A Halide-Based Fast Sodium-Ion Conductor with Vacancy-Driven Ionic Transport. *ACS Applied Energy Materials* **2020**, *3*, 10164-10173.
- 10. Hu, Y.; Fu, J.; Xu, J.; Luo, J.; Zhao, F.; Su, H.; Liu, Y.; Lin, X.; Li, W.; Kim, J. T.; Hao, X.; Yao, X.; Sun, Y.; Ma, J.; Ren, H.; Yang, M.; Huang, Y.; Sun, X., Superionic amorphous NaTaCl₆ halide electrolyte for highly reversible all-solid-state Na-ion batteries. *Matter* **2024**, *7*, 1018-1034.
- 11. Tanaka, Y.; Ueno, K.; Mizuno, K.; Takeuchi, K.; Asano, T.; Sakai, A., New Oxyhalide Solid Electrolytes with High Lithium Ionic Conductivity >10 mS cm⁻¹ for All-Solid-State Batteries. *Angew. Chem. Int. Ed.* **2023**, *62*, e202217581.
- 12. Lin, X.; Zhao, Y.; Wang, C.; Luo, J.; Fu, J.; Xiao, B.; Gao, Y.; Li, W.; Zhang, S.; Xu, J.; Yang, F.; Hao, X.; Duan, H.; Sun, Y.; Guo, J.; Huang, Y.; Sun, X., A Dual Anion Chemistry-Based Superionic Glass Enabling Long-Cycling All-Solid-State Sodium-Ion Batteries. *Angew. Chem. Int. Ed.* **2023**, *136*, e202314181.
- 13. Grazulis, S.; Chateigner, D.; Downs, R. T.; Yokochi, A. F. T.; Quiros, M.; Lutterotti, L.; Manakova, E.; Butkus, J.; Moeck, P.; Le Bail, A., Crystallography Open Database an openaccess collection of crystal structures. *J. Appl. Crystallogr.* **2009**, *42*, 726-729.

- 14. Ishiguro, Y.; Ueno, K.; Nishimura, S.; Iida, G.; Igarashib, Y., TaCl5-glassified Ultrafast Lithium Ion-conductive Halide Electrolytes for High-performance All-solid-state Lithium Batteries. *Chem. Lett.* **2023**, *52*, 237-241.
- 15. Billinge, S. J. L., The rise of the X-ray atomic pair distribution function method: a series of fortunate events. *Philosophical Transactions of the Royal Society A: Mathematical, Physical and Engineering Sciences* **2019**, *377*, 20180413.
- 16. Carlson, G. L., Vibrational spectra of some *MCl*₅ molecules: SbCl₅, PCl₅, TaCl₅ and NbCl₅. *Spectrochim. Acta* **1963**, *19*, 1291-1307.
- 17. Nour, E. M., Vibrational analysis of the trigonal bipyramidal NbCl₅ and NbBr₅ molecules. *Spectrochim. Acta, Pt. A: Mol. Spectrosc.* **1986,** *42*, 1411-1414.
- 18. Sakowski-Cowley, A. C.; Lukaszewicz, K.; Megaw, H. D., The structure of sodium niobate at room temperature, and the problem of reliability in pseudosymmetric structures. *Acta Cryst. B* **1969,** *25*, 851-865.
- 19. Hardcastle, F. D.; Wachs, I. E., Determination of niobium-oxygen bond distances and bond orders by Raman spectroscopy. *Solid State Ion.* **1991**, *45*, 201-213.
- 20. Zhang, S.; Zhao, F.; Chen, J.; Fu, J.; Luo, J.; Alahakoon, S. H.; Chang, L.-Y.; Feng, R.; Shakouri, M.; Liang, J.; Zhao, Y.; Li, X.; He, L.; Huang, Y.; Sham, T.-K.; Sun, X., A family of oxychloride amorphous solid electrolytes for long-cycling all-solid-state lithium batteries. *Nature Communications* **2023**, *14*, 3780.
- 21. Sebti, E.; Qi, J.; Richardson, P. M.; Ridley, P.; Wu, E. A.; Banerjee, S.; Giovine, R.; Cronk, A.; Ham, S.-Y.; Meng, Y. S.; Ong, S. P.; Clément, R. J., Synthetic control of structure and conduction properties in Na–Y–Zr–Cl solid electrolytes. *Journal of Materials Chemistry A* **2022**, *10*, 21565-21578.
- 22. Ridley, P.; Nguyen, L. H. B.; Sebti, E.; Han, B.; Duong, G.; Chen, Y.-T.; Sayahpour, B.; Cronk, A.; Deysher, G.; Ham, S.-Y.; Oh, J. A. S.; Wu, E. A.; Tan, D. H. S.; Doux, J.-M.; Clément, R.; Jang, J.; Meng, Y. S., Amorphous and nanocrystalline halide solid electrolytes with enhanced sodium-ion conductivity. *Matter* **2024**, *7*, 485-499.
- 23. Brug, G. J.; van den Eeden, A. L. G.; Sluyters-Rehbach, M.; Sluyters, J. H., The analysis of electrode impedances complicated by the presence of a constant phase element. *Journal of Electroanalytical Chemistry and Interfacial Electrochemistry* **1984**, *176*, 275-295.
- 24. Irvine, J. T. S.; Sinclair, D. C.; West, A. R., Electroceramics: Characterization by Impedance Spectroscopy. *Adv. Mater.* **1990,** *2*, 132-138.
- 25. Kwak, H.; Lyoo, J.; Park, J.; Han, Y.; Asakura, R.; Remhof, A.; Battaglia, C.; Kim, H.; Hong, S.-T.; Jung, Y. S., Na2ZrCl6 enabling highly stable 3 V all-solid-state Na-ion batteries. *Energy Storage Materials* **2021**, *37*, 47-54.
- 26. Zhao, T.; Sobolev, A. N.; Martinez de Irujo Labalde, X.; Kraft, M. A.; Zeier, W. G., On the influence of the coherence length on the ionic conductivity in mechanochemically synthesized sodium-conducting halides, Na3-xIn1-xZrxCl6. *Journal of Materials Chemistry A* **2024**, *12*, 7015-7024.
- 27. Zhao, T.; Sobolev, A. N.; Schlem, R.; Helm, B.; Kraft, M. A.; Zeier, W. G., Synthesis-Controlled Cation Solubility in Solid Sodium Ion Conductors Na2+xZr1-xInxCl6. *ACS Applied Energy Materials* **2023**, *6*, 4334-4341.
- 28. Zhao, T.; Kraft, M. A.; Zeier, W. G., Synthesis-Controlled Polymorphism and Anion Solubility in the Sodium-Ion Conductor Na3InCl6–xBrx ($0 \le x \le 2$). *lnorg. Chem.* **2023**, *62*, 11737-11745.
- 29. Wang, X.; Chen, J.; Mao, Z.; Wang, D., Effective resistance to dendrite growth of NASICON solid electrolyte with lower electronic conductivity. *Chem. Eng. J.* **2022**, *427*, 130899.

- 30. Shao, B.; Huang, Y.; Han, F., Electronic Conductivity of Lithium Solid Electrolytes. *Advanced Energy Materials* **2023**, *13*, 2204098.
- 31. Wenzel, S.; Leichtweiss, T.; Weber, D. A.; Sann, J.; Zeier, W. G.; Janek, J., Interfacial Reactivity Benchmarking of the Sodium Ion Conductors Na3PS4 and Sodium β-Alumina for Protected Sodium Metal Anodes and Sodium All-Solid-State Batteries. *ACS Applied Materials & Interfaces* **2016**, *8*, 28216-28224.
- 32. Riegger, L. M.; Schlem, R.; Sann, J.; Zeier, W. G.; Janek, J., Lithium-Metal Anode Instability of the Superionic Halide Solid Electrolytes and the Implications for Solid-State Batteries. *Angew. Chem. Int. Ed.* **2021**, *60*, 6718-6723.
- 33. Wenzel, S.; Leichtweiss, T.; Krüger, D.; Sann, J.; Janek, J., Interphase formation on lithium solid electrolytes—An in situ approach to study interfacial reactions by photoelectron spectroscopy. *Solid State Ionics* **2015**, *278*, 98-105.
- 34. Jain, A.; Ong, S. P.; Hautier, G.; Chen, W.; Richards, W. D.; Dacek, S.; Cholia, S.; Gunter, D.; Skinner, D.; Ceder, G.; Persson, K. A., Commentary: The Materials Project: A materials genome approach to accelerating materials innovation. *APL Materials* **2013**, *1*, 011002.